Key Laboratory of Forest Plant Ecology, Northeast Forestry University, Harbin City, China

Characterization and pharmacokinetics of coenzyme Q_{10} nanoparticles prepared by a rapid expansion of supercritical solution process

XIANGDONG MENG, YUANGANG ZU, XIUHUA ZHAO, QINGYONG LI, SHOUGANG JIANG, MEI SANG

Received June 17, 2011, accepted August 1, 2011

Yuangang Zu, Key Laboratory of Forest Plant Ecology, Northeast Forestry University, No26 Hexing Road, Harbin City, Heilongjiang Province, 150040, China
zuyuangang@163.com

Pharmazie 67: 161–167 (2012) *doi: 10.1691/ph.2012.1086*

Coenzyme Q_{10} (CoQ_{10}) has been found to be effective in cardiovascular diseases and neurodegenerative diseases. However, the extremely poor solubility of CoQ_{10} in water is hampering its bioavailability as a therapeutic agent. To overcome solubility problem, we micronized the CoQ_{10} powder to the nanometer level by the supercritical solution (RESS) process, which does not employ any toxic organic solvent. The obtained CoQ_{10} nanoparticles were 147.9 ± 27.3 nm in diameter and their physicochemical properties were characterized by scanning electron microscopy (SEM), dynamic light scattering (DLS), liquid chromatography–mass spectrometry (LC–MS), X-ray diffractometry (XRD) and differential scanning calorimetry (DSC) analyzes. Moreover, the pharmacokinetics of the CoQ_{10} nanoparticles, in comparison with the unprocessed CoQ_{10} powder, were investigated in rats. From the results of physicochemical and pharmacokinetic studies, the CoQ_{10} nanoparticles had high solubility in water and possessed less crystalline structure, which can enhance the bioavailability of CoQ_{10}, and provide a water-soluble solid dosage form of CoQ_{10}.

1. Introduction

Coenzyme Q_{10} (CoQ_{10}), an extremely water-insoluble antioxidant, is found in the membranes of many organelles. It is a membrane stabilizer and plays a key role in mitochondrial oxidative phosphorylation and ATP production (Thanatuksorn et al. 2009). In addition to scavenging free radicals directly, CoQ_{10} regenerates tocopherol which acts as an antioxidant that protects membrane phospholipids and proteins from lipid peroxidation (Pepe et al. 2007). Due to its apparently nontoxic nature, CoQ_{10} has been drawn to possible clinical and therapeutic uses. In early clinical trials, health benefits of CoQ_{10} supplementation relate to cardiovascular diseases have been reported in a large number of studies, where CoQ_{10} has been used as an adjunct to standard medical therapy (Li et al. 2008). In recent years, CoQ_{10} has been tested as a therapeutic agent for neurodegenerative diseases such as Parkinson's, Huntington's and mitochondrial diseases. However, the lipophilic property of CoQ_{10} renders it poorly absorbed when taken orally by humans. The low oral bioavailability of CoQ_{10} could be a difficulty in administering this molecule to achieve therapeutic concentrations (Ankola et al. 2007).

To overcome the solubility problem, some CoQ_{10} analogs have been synthesized. These analogs could improve the stability of CoQ_{10} in the products, but did not enhance bioavailability (Gao et al. 2006). In the past few years, some novel delivery systems of CoQ_{10} have been developed, including liposomes (Lee et al. 2010; Zhang et al. 2009), nanostructured lipid carriers (Pardeike et al. 2010; Teeranachaideekul et al. 2007), polymeric nanoparticles (Kwon et al. 2002; Nehilla et al. 2008), solid dispersions (Nepal et al. 2010) and self-emulsifying drug delivery systems (SEDDS) (Kang et al. 2004; Kommuru et al. 2001; Palamakula et al. 2004). These delivery systems were based on coating CoQ_{10} with biodegradable polymeric materials. Although some of the formulations have been confirmed to have a higher oral bioavailability of CoQ_{10} than that of standard commercial products, they were limited in clinical trials because of biodegradable polymers that remain unclear in the health effects for humans. Thus, there continues to be a need to develop improved formulations for the oral delivery of CoQ_{10} without the possible toxic effects.

Micronization of CoQ_{10} powder into particles in submicron level is an approach that may overcome these challenges by increasing the surface area available for dissolution. The application of supercritical fluids for the precipitation of pharmaceuticals and natural substances has attracted great attention. Rapid expansion of supercritical solution (RESS), which does not employ toxic organic solvents, is a well-recognized process for the micronization. The major advantage of the RESS process is the production of pure particles in micron and submicron levels controlled by the RESS processing parameters using a mathematical model (Byrappa et al. 2008). In this process, the solute is dissolved in a supercritical fluid, and then passed through a nozzle at supersonic speed. Pressure reduction of solution in a nozzle leads to a rapid expansion. The RESS process is applicable to substances soluble in supercritical fluids. Carbon dioxide is the most commonly used supercritical fluid due to its non-toxicity and low critical temperature. The solubility of CoQ_{10} in supercritical CO_2 is ranging from 0.1 to 1.97 g/L under different pressure and tempearture (Ana et al. 2004), so the RESS process is a promising method to reduce the particle size and improve the bioavailability of CoQ_{10}.

To our best knowledge, micronization of CoQ_{10} using RESS process has not been reported. Therefore, the first goal of this work was to study the feasibility of CoQ_{10} micronization by a RESS process. Orthogonal array design method has been applied to

explore the optimal conditions of RESS process. In addition, the obtained CoQ_{10} particles were characterized by scanning electron microscopy (SEM), dynamic light scattering (DLS), liquid chromatography–mass spectrometry (LC–MS), X-ray diffractometry (XRD) and differential scanning calorimetry (DSC) to characterize the physicochemical properties of the micronized particles. Then, to confirm the usefulness of the CoQ_{10} nanoparticles in improving oral bioavailability, an *in vivo* absorption study was carried out in rats compared with the unprocessed CoQ_{10} powder.

2. Investigations, results and discussion

2.1. Optimization of the RESS process

In the present study, the optimization of suitable operating conditions in RESS was examined using an orthogonal OA_{16} (4) [4] test design. The experimental assignment and collected data for micronized CoQ_{10} particle sizes is shown in Table 1. The data are analyzed using Design Expert 7.0 software for evaluating the effect of each parameter on the optimization criteria. The results presented in Table 1 indicate a maximum MPS of micronized CoQ_{10} of 299.6 ± 48.3 nm, and a minimum of 151.7 ± 29.1 nm. It can be concluded from Table 1 that the influence to the MPS of micronized CoQ_{10} decreases in the order: A > C > B > D according to the R-values. The minimum particle size of micronized CoQ_{10} was obtained under $A_4B_2C_2D_1$ (25 Mpa of extraction pressure, 40 °C of extraction temperature, 200 μm of nozzle diameter, and 25 °C of precipitation temperature). Through a confirmatory test, smaller micronized CoQ_{10} was got, with a MPS of 147.9 ± 27.3 nm.

2.2. Characterization of CoQ10 nanoparticles

2.2.1. Solubility in water

Figure 1 shows the photographs of unprocessed CoQ_{10} powder and CoQ_{10} nanoparticles dispersed in water. Unprocessed CoQ_{10} powder could not be dispersed in water. However, the suspension of CoQ_{10} nanoparticles was a homogenous yellow color and remained stable for over 8 h without any discernible sedimentation. The solubility of CoQ_{10} nanoparticles in water determined by HPLC was 0.19 mg of CoQ_{10} per mL. However, the water solubility of unprocessed CoQ_{10} powder was found to be very low (0.4 μg of CoQ_{10} per mL). The results showed that CoQ_{10} nanoparticles have high solubility in water.

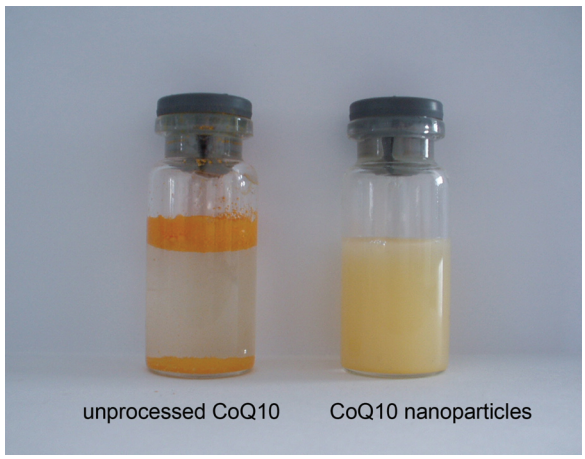

Fig. 1: CoQ10 nanoparticles and unprocessed CoQ10 dissolved into water at the concentration of 1 mg/mL

2.2.2. Surface morphology

To obtain the information about the shapes of particles, SEM analysis was performed with unprocessed CoQ_{10} powder and CoQ_{10} nanoparticles, and SEM images were shown in Fig. 2. The unprocessed CoQ_{10} powder consisted of some large lamelliform crystals (10–20 μm), which might be generated due to any size reducing processes in the course of manufacturing. CoQ_{10} nanoparticles were non-spherical shaped particles with smaller size ranging from 100 to 200 nm. A previous study investigated the effects of operating parameters on the particles formation (Charpentier et al. 2008). They showed that a low concentration induces formation of spherical nanoparticles with a narrow size distribution. In the present study, CoQ10 nanoparticles were produced by higher concentration (the solubility of CoQ_{10} in supercritical CO_2 is 1.84 g/L under operating conditions). This could be a part of reasons why CoQ_{10} nanoparticles exhibited non-spherical morphology.

2.2.3. Particle size and zeta-potential in aqueous solution

After the addition of CoQ_{10} nanoparticles into water, it was found to form a homogeneous aqueous solution with a mean diameter of 147.9 ± 27.3 nm and Zeta potential (ZP) of -34.4 ± 2.3 mV. The polydispersity value (0.168 ± 0.015) of CoQ_{10} nanoparticles was lower than 0.2 indicating a relatively narrow size distribution, as shown in Fig. 3. On the contrary, unprocessed CoQ_{10} powder exhibited extremely insolubility in water, and could not be measured by DLS because the measurement range was too narrow (1 nm to 6 μm). It is evident

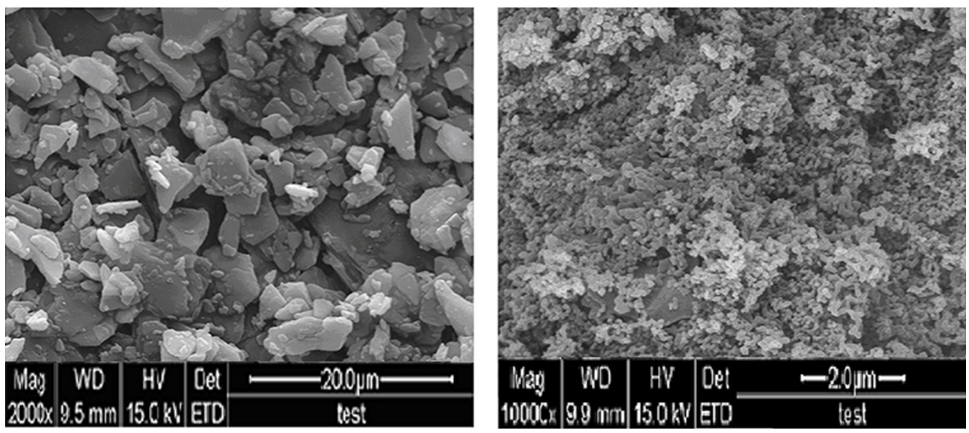

(a) (b)

Fig. 2: SEM images of unprocessed CoQ10 powder (a) and CoQ10 nanoparticles (b)

Table 1: Orthogonal array design OA16 (4) 4 and experimental results

Trail no.	A (MPa)	B (°C)	C (μm)	D (°C)	Solubilities of CoQ_{10} in supercritical CO_2 (g/L)	MPS (nm) ± S.D. (n = 3)
1	1(10)	1(35)	1(100)	1(25)	0.07	299.6 ± 48.3
2	1(10)	2(40)	2(200)	2(30)	0.09	215.4 ± 40.6
3	1(10)	3(45)	3(300)	3(35)	0.12	176.0 ± 35.9
4	1(10)	4(50)	4(400)	4(40)	0	168.5 ± 34.4
5	2(15)	1(35)	2(200)	3(35)	0.32	164.8 ± 33.9
6	2(15)	2(40)	1(100)	4(40)	0.41	205.9 ± 38.9
7	2(15)	3(45)	4(400)	1(25)	0.57	152.3 ± 29.2
8	2(15)	4(50)	3(300)	2(30)	0.14	159.8 ± 30.1
9	3(20)	1(35)	3(300)	4(40)	0.79	168.5 ± 35.4
10	3(20)	2(40)	4(400)	3(35)	1.02	153.5 ± 28.6
11	3(20)	3(45)	1(100)	2(30)	1.26	185.4 ± 36.5
12	3(20)	4(50)	2(200)	1(25)	0.54	162.9 ± 35.9
13	4(25)	1(35)	4(400)	2(30)	1.11	157.5 ± 29.7
14	4(25)	2(40)	3(300)	1(25)	1.87	151.7 ± 29.1
15	4(25)	3(45)	2(200)	4(40)	1.68	158.7 ± 35.9
16	4(25)	4(50)	1(100)	3(35)	1.53	166.6 ± 35.7
K1a	214.7 ± 39.9	189.6 ± 37.1	215.4 ± 39.1	162. 5 ± 35.2		
K2	165.7 ± 35.3	154.6 ± 33.7	158.7 ± 32.2	175.3 ± 36.1		
K3	152.6 ± 34.2	157. 5 ± 34.6	163.8 ± 35.8	168.9 ± 35.7		
K4	149.9 ± 28.8	176.5 ± 36.2	162.4 ± 34.5	170.9 ± 35.8		
Rb	74.8	45.0	67.4	12.8		
Optimal level	A4	B2	C2	D1		

a $KiA = \sum$(mean particle size at Ai)/4, the mean values of mean particle size for a certain factor at each level with standard deviation. b $RiA = \max\{KiA\} - \min\{KiA\}$. A: extraction pressure; B: extraction temperature; C: nozzle diameter; D: precipitation temperature; MPS: mean particle size

that a decrease of the particle size down to the nanometer range will increase dissolution rate due to the increase of the effective particle surface area (Patravale et al. 2004). The CoQ_{10} nanoparticles with greatly enhanced particle surface area that is generated by RESS process lead to enhance the dissolution rate of the poorly water-soluble CoQ_{10} powder. The ZP values can reflect the electric charge on the particle surface and indicate the physical stability of colloidal systems. ZP values higher than -30 mV show good physical stability. In the present study, the ZP values of micronized CoQ_{10} particles were -34.4 ± 2.3 mV, indicating that micronized CoQ_{10} particles should possess good physical stability.

2.2.4. LC–MS, XRD and DSC analysis

Figure 4 shows LC–MS spectra of unprocessed and processed CoQ_{10}. After processed, CoQ_{10} exhibits an unchanged molecular weight (at m/z 864.0). The result suggests that no varieties about chemistry structure of CoQ_{10} before/after RESS process occur. Therefore, the RESS process has not induced degradation of CoQ_{10}. To characterize the degree of crystallinity of the CoQ_{10} nanoparticles, XRD analysis was performed. According to the XRD patterns (Fig. 5), a sharp and intense peak observed at 18° (2θ) should be characteristic and helpful for identifying crystalline conditions. Interestingly, a significant reduction of this peak was confirmed in CoQ_{10} nanoparticles. This fact suggests that CoQ_{10} particles after RESS processing are less crystalline. In addition to XRD analysis, particles were subjected to DSC analysis for further elucidation of the crystal conditions. DSC results provide useful information about the physical and chemical changes in heat capacity. As shown in Fig. 6, the DSC profile of unprocessed CoQ_{10} powder shows an endothermic melting peak at 49.56 °C, whereas, the intensity of the endothermic peak in CoQ_{10} nanoparticles was 45.97 °C. The decrease of melting enthalpy recorded by DSC analysis of micronized CoQ_{10} particles is in agreement with the decrease of peak intensity observed by XRD, indicating a less crystal structure. Therefore, taken together with the preparation of CoQ_{10} nanoparticles, the present findings suggest that RESS process could be effective in manufaturing CoQ_{10} nanoparticles, which have smaller particle sizes and less crystalline structure compared with unprocessed CoQ_{10} powder.

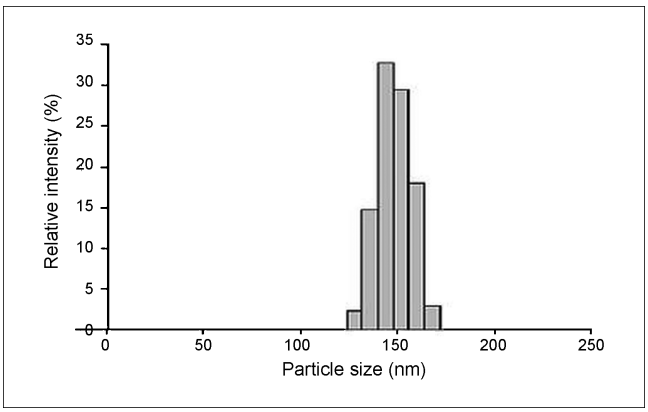

Fig. 3: Particle size distribution of CoQ10 nanoparticles

2.3. Improvement of bioavailability

An *in vivo* absorption study was undertaken with unprocessed CoQ_{10} powder and CoQ_{10} nanoparticles dispersed in water to determine whether the CoQ_{10} nanoparticles could increase the absorption after oral administration in rats. Plasma concentration *versus* time curves of unprocessed CoQ_{10} powder and CoQ_{10} nanoparticles following oral (50 mg/kg) administration are depicted in Fig. 7. CoQ_{10} level in the blood of rats treated with unprocessed CoQ_{10} powder was found to be very low, but CoQ_{10} nanoparticles were absorbed rapidly. According to the pharmacokinetic parameters (Table 2), improvement of C_{max} and AUC_{0-12h} was observed in CoQ_{10} nanoparticles as compared to unprocessed CoQ_{10} powder. The T_{max} of CoQ_{10} nanoparticles (3 h) is shorter than that of unprocessed CoQ_{10} powder with 4 h,

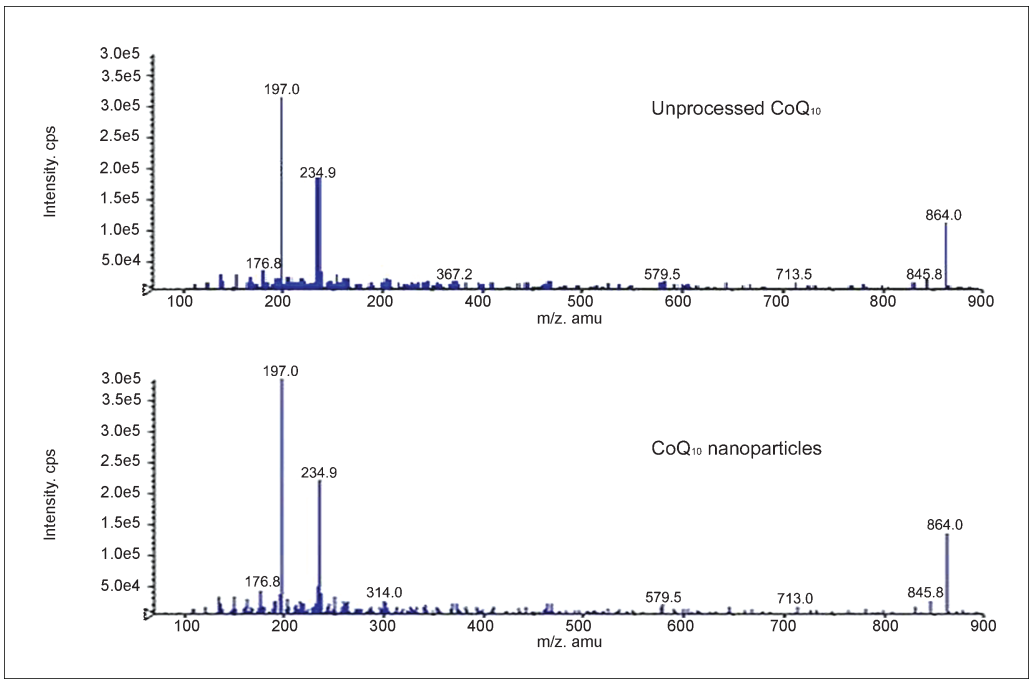

Fig. 4: LC-MS spectra of CoQ10 nanoparticles and unprocessed CoQ10 powder

Table 2: Comparison of pharmacokinetic parameters of unprocessed CoQ10 powder and micronized CoQ10 particles after an oral does of 50 mg/kg in rats

Parameters Formulations	T_{max} (h)	C_{max} (ng/mL)	AUC_{0-12h} (ng·h/mL)	$t_{1/2}$ (h)
Unprocessed CoQ_{10}	4	76.4 ± 12.8	538.2 ± 95.6	4.82 ± 0.19
CoQ_{10} nanoparticles	3	175.6 ± 27.5*	1140.3 ± 229.4*	3.55 ± 0.14

Values are expressed as means ± S.D. T_{max}: Time of maximal plasma concentration; C_{max}: Maximal plasma concentration; AUC_{0-12h}: Area under the concentration-time curve from 0 to the last time point; $t_{1/2}$: Apparent terminal rate constant. *$P < 0.05$ vs. unprocessed CoQ_{10}

showing that the absorption rate of CoQ_{10} is increased. There was no statistical difference in $t_{1/2}$ between unprocessed CoQ_{10} powder and CoQ_{10} nanoparticles ($P > 0.05$), which suggests the time for CoQ_{10} nanoparticles remaining in the body was not significantly variational. AUC_{0-12h} of micronized CoQ_{10} particles is 1.96-fold higher than that of unprocessed CoQ_{10} powder, indicating that oral absorption of CoQ_{10} is enhanced strongly by micronized CoQ_{10} particles ($P < 0.05$ vs. unprocessed CoQ_{10}). It is known that a size exclusion phenomenon exists in the gastrointestinal absorption of particles, with 100 nm particles showing a significantly higher uptake than larger particles (500 nm to 10 μm) (Desai et al. 1996). Besides particle size, drug crystallinity plays a key role in drug absorption of solid dosage forms. There are a number of literature reports which have demonstrated improving dissolution performance in the polymorphic form (Kobayashi et al. 2000; Tian et al. 2007). Therefore, the

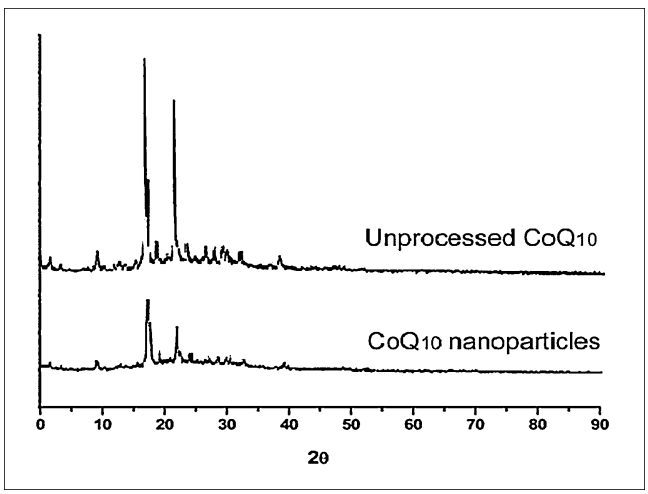

Fig. 5: X-ray diffraction patterns of CoQ10 nanoparticles and unprocessed CoQ10 powder

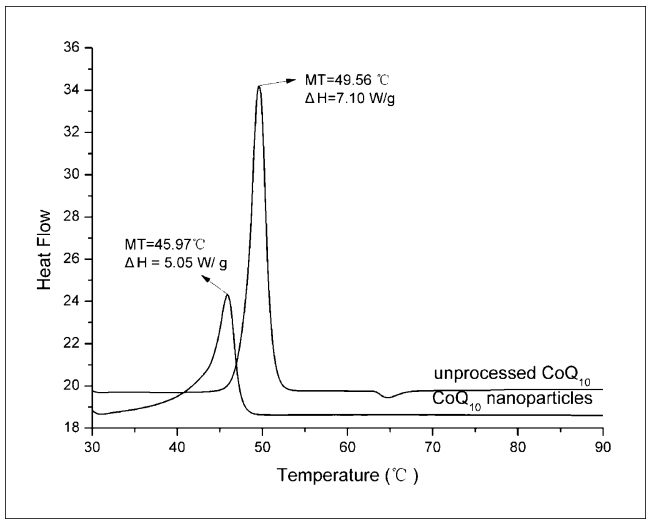

Fig. 6: Thermographs of CoQ10 nanoparticles and unprocessed CoQ10 powder by differential scanning calorimetry. MT: melting temperature; ΔH: heat of fusion

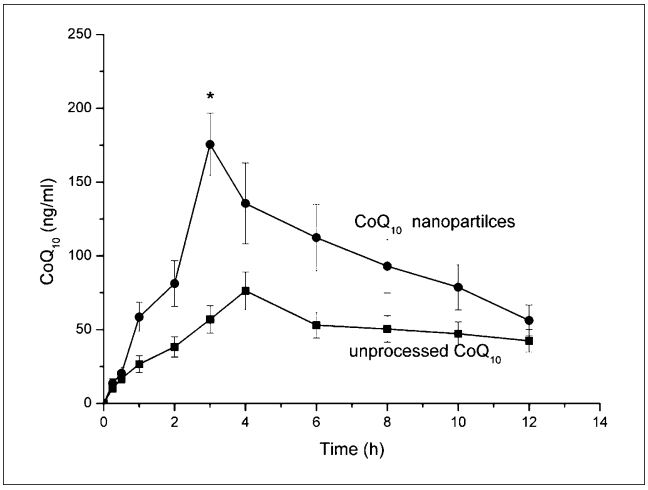

Fig. 7: Plasma concentration-time curves after an oral administration of CoQ10 nanoparticles and unprocessed CoQ10 powder at the dose of 50 mg CoQ10 eq./kg in rats. Data points represent as means ± S.D. (n = 6). *$P < 0.05$ vs. unprocessed CoQ10

small size and less crystalline structure of the micronized CoQ_{10} particles could improve the dissolution result in an improved adsorption into the intestinal epithelial cells, which may explain the dramatic increase in CoQ_{10} absorption.

The absorption efficiency of orally ingested CoQ_{10} is poor because of its insolubility in water. It has been reported that in rats only 2–3% of orally administered CoQ_{10} is absorbed (Zhang et al. 1995). Previously, various approaches to enhance solubility and bioavailability of CoQ_{10} had been reported in the literature, including solid dispersions, liposomes, nanostructured lipid carriers, polymeric nanoparticles and SEDDS. Solid dispersions, liposomes and nanostructured lipid carriers showed improved CoQ_{10} solubility, however, without information on enhanced bioavailability of CoQ_{10}. The employment of polymeric nanoparticles showed less improvement in the bioavailability of CoQ_{10}. A study demonstrated about 1.1 times improvement in AUC from CoQ_{10} coated γ-cyclodextrin complex over crystalline CoQ_{10} in human (Terao et al. 2006). The use of SEDDS seemed to be a useful strategy for improving bioavailability of CoQ_{10}. A research study reported a two-fold increase in the bioavailability from the SEDDS of CoQ_{10} when compared with CoQ_{10} alone in male rats (Palamakula et al. 2004). However, CoQ_{10} was found to be easily oxidized and sensitive to light, leading to rapid photodegradation, especially the liquid-state CoQ_{10} was found to be far more prone to photodegradation than the solid sample (Hatanaka et al. 2008). Herein, CoQ_{10} nanoparticles produced by RESS process might be a more suitable strategy for overcoming solubility and bioavailability problems of CoQ_{10}.

3. Experimental

3.1. Materials

CoQ_{10} was purchased from Xi'an Hao Tian Bio-engineering Technology Inc (Xi'an, PR China). CoQ_{10} is a yellow powder crystal obtained with purities beyond 98%. High purity CO_2 (99.99%) was purchased from Liming Gas Company of Harbin (Heilongjiang, PR China). CoQ_9 standard was purchased from Sigma-Aldrich Inc (St. Louis, MO, USA). Ethanol and methanol were HPLC grade (Hurdick & Jackson, USA). All other chemicals were of analytical grade.

3.2. Preparation of micronized CoQ_{10} nanoparticles

The RESS apparatus, designed and made by our laboratory, was shown schematically in Fig. 8. Briefly, CoQ_{10} powder was put in the form of powder in the extraction chamber, and was then dissolved in supercritical CO_2 fluid. The CoQ_{10}/CO_2 solution was sprayed rapidly through a nozzle into a precipitating chamber from a desired pressure to atmospheric pressure. CoQ_{10} nanoparticles were collected in the expansion chamber. Since various parameters potentially affect particle size, the optimization of the experimental conditions is a critical step to develop a RESS method. In fact, extraction pressure, extraction temperature, nozzle diameter and precipitation temperature are generally considered the most important factors. An orthogonal design OA_{16} $(4)^4$ was selected for optimization of operating condition of CoQ_{10} micronization by RESS process. The RESS experiments were carried out with 4 factors and 4 levels, including extraction pressure (10, 15, 20, 25 MPa), extraction temperature (35, 40, 45, 50 °C), nozzle diameter (100, 200, 300, 400 μm), and precipitation temperature (25, 30, 35, 40 °C). The range of each factor level is based on the results of preliminary experiments. The mean particle size (MPS) of micronized CoQ_{10} particles is the dependent variable. The data are analyzed using the Design Expert 7.0 software. The significance level is stated at 95%, with P-value 0.05.

3.3. Characterization of micronized CoQ_{10} nanoparticles

3.3.1. Solubility in water

A 10 mg sample (unprocessed CoQ10 powder and CoQ10 nanoparticles) was added to 10 mL distilled water. The samples were stirred at 500 rpm using magnetic stirrer at 37 °C for 30 min. The suspensions were filtrated through a membrane filter (Milipore Millex-HV PVDF, 0.45 μm) and suitably diluted with ethanol and analyzed for CoQ10 concentration by HPLC. Briefly, CoQ10 was quantified by Diode Array Detector (Waters Company, USA) following HIQ SIL C18 V column (ø 4.6 mm × 250 mm, KYA TECH Corporation, Japan) separation at 275 nm. The mobile phase was ethanol-methanol (90:10, v/v) containing 1.0% acetic acid. Flow rate and injection volume were 1.0 mL/min and 20 μL. The running time was 8.5 min. The experiment was performed in triplicates.

3.3.2. Surface morphology

The surface morphological characteristics of unprocessed CoQ_{10} powder and CoQ_{10} nanoparticles were examined using SEM (Quanta 200, FEI). Prior to analysis, samples were diluted with distilled water, dropped on the amorphous carbon grid, and then air-dried at room temperature.

3.3.3. Particle size and zeta-potential in aqueous solution

Particle size, zeta-potential and polydispersity index (PI) analysis were performed with DLS (ZetaPALS/90plus, Brookhaven Instruments) particle size analyzer. Prior to measurement, 0.1 g of unprocessed CoQ_{10} powder and CoQ_{10} nanoparticles was diluted with 10 mL distilled water and dispersed homogeneously. MPS was calculated using the photon correlation from light scattering. Zeta-potential was calculated using the Smolchowski equation from the electrophoresis mobility and electric field strength. Every measurement was repeated at least three times. PI was calculated as the ratio between the weight and number average molecular weights, and is a measure of the width of the particle size distribution.

3.3.4. LC–MS analysis

The unprocessed CoQ_{10} powder and CoQ_{10} nanoparticles were dissolved in ethanol separately. LC–MS spectra were obtained by Analyst Software version 1.4 of API 3000 (Applied Biosystems, USA). The mass spectrometer was operated in positive ion mode.

3.3.5. X-ray diffraction analysis (XRD)

X-ray diffraction patterns were collected in transmission using an X-ray diffractometer with a rotating anode (Philips, Xpert-Pro, Netherlands) with Cu Kα radiation generated at 30 mA and 40 kV. The unprocessed CoQ_{10} powder and CoQ_{10} nanoparticles were filled to the same depth inside the sample holder by leveling with spatula and scanning rate (2 °/min) was the same for all XRD analysis.

3.3.6. Differential scanning calorimetry (DSC)

To evaluate crystallinity of unprocessed CoQ_{10} powder and CoQ_{10} nanoparticles, thermal analysis was carried out using DSC (TA instruments, model DSC 204). 5 mg of sample was placed in a sealed aluminum pan at a scanning rate of 5 °C/min from 30 to 90 °C. An empty aluminum pan was used as a reference.

3.4. Pharmacokinetic studies in rats

3.4.1. Animals and study design

The pharmacokinetic studies were carried out in Wistar rats. Male Wistar rats (200–250 g) were obtained from the Central Animal House, Chinese

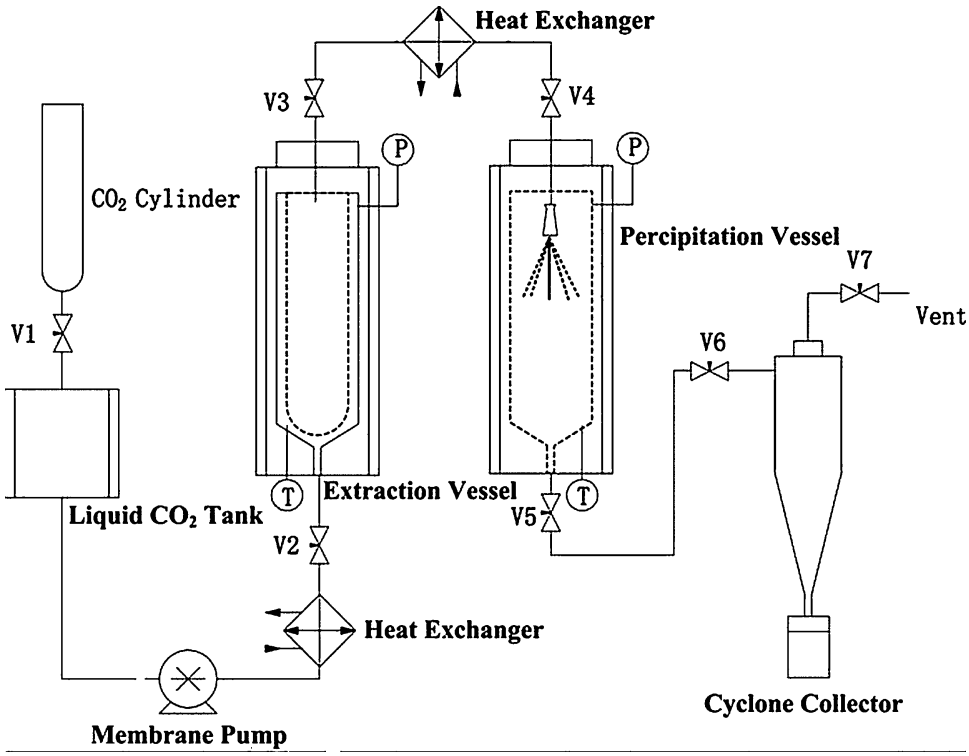

Fig. 8: Schematic diagram of the RESS process

Academy of Science, Shanghai. The animals were randomly assigned to two groups of 18 rats, and each group was randomly divided into three subgroups of six rats each. The test substances were orally administered after rats were deprived of food for 16 h. Rats received unprocessed CoQ_{10} powder or CoQ_{10} nanoparticles at the dose of 50 mg/kg. Blood samples were collected at 0, 0.25, 0.5, 1, 2, 3, 4, 6, 8, 10 and 12 h from retro-orbital plexus into microtubes containing the anti-coagulant after dosing.

3.4.2. *Measurement of CoQ_{10} concentration in plasma in rats*

Plasma was obtained immediately and processed by protein precipitation. The blood samples (0.4 mL) were treated by centrifugation at 3000 rpm for 15 min. Supernatant liquor plasma sample (0.2 mL) was kept and supplemented with 25 μL of CoQ_9 (10 μg/mL) as an internal standard. The samples were mixed with 0.4 mL ethanol and vortexed for 10 s, and then 5 mL hexane was added, followed by vortexing for 5 min and centrifugation (3000 rpm, 10 min). The organic layer was collected and evaporated to dryness under nitrogen. The sample residues were dissolved in mobile phase and subjected to HPLC analysis for determination of CoQ_{10} content. The HPLC method was mentioned above in the Section 3.3.2. All samples were preformed in triplicate.

3.4.3. *Statistical analysis*

All the means are presented with their standard deviation (mean ± S.D.). The pharmacokinetic parameters of unprocessed CoQ_{10} powder and CoQ_{10} nanoparticles treated groups were compared using one-way ANOVA, followed by post hoc Dunnett test. An unpaired Student's *t*-test was used to determine the significant difference between the pharmacokinetic parameters of unprocessed CoQ_{10} powder and CoQ_{10} nanoparticles treated groups. $P < 0.05$ was considered statistically significant. The area under the drug concentration-time curve from time 0 to 12 h (AUC_{0-12h}) was calculated by using Sigma Plot® 10.0, SPSS scientific graphing software (SPSS Inc., Chicago, IL, USA). The maximal plasma concentration of drug (C_{max}) and the time to reach maximum plasma concentration (T_{max}) were directly obtained from plasma data. The elimination rate constant (Kel) was obtained from the terminal slope using regression analysis, and the half-life ($t_{1/2}$) of the drug was calculated by a relationship of 0.693/Kel.

Acknowledgments: This work was supported by the Special Fund for Forestry Scientific Research in the Public Interest (2010040072), 948 Project of the State Forestry Administration of China (2010–4-20) and Heilongjiang Postdoctoral Grant (LBH-10283).

References

Ana AM, Ana VMN, Teresa C, Catarina MMD (2004) Solubility of coenzyme Q10 in supercritical carbon dioxide. J Supercritical Fluids 28: 201–206.

Ankola DD, Viswanad B, Bhardwaj V, Ramarao P, Kumar MN (2007) Development of potent oral nanoparticulate formulation of coenzyme Q10 for treatment of hypertension: Can the simple nutritional supplements be used as first line therapeutic agents for prophylaxis/therapy? Eur J Pharm Biopharm 67: 361–369.

Byrappa K, Ohara S, Adschiri T (2008) Nanoparticles synthesis using supercritical fluid technology-towards biomedical applications. Adv Drug Deliv Rev 60: 299–327.

Charpentier PA, Jia M, Lucky RA (2008) Study of the RESS process for producing beclomethasone-17, 21-dipropionate particles suitable for pulmonary delivery, AAPS Pharm Sci Tech 9: 39–46.

Desai MP, Labhasetwar V, Amidon GL, Levy RJ (1996) Gastrointestinal uptake of biodegradable microparticles: effect of particle size. Pharm Res 13: 1838–1845.

Hatanaka J, Kimura Y, Lai-Fu Z, Onoue S, Yamada S (2008) Physicochemical and pharmacokinetic characterization of water-soluble Coenzyme Q10 formulations. Int J Pharm 363: 112–117.

Gao XY, Nishimura K, Hirayama F, Arima H, Uekama K, Schmid G, Terao K, Nakata D, Fukumi H (2006) Enhanced dissolution and oral bioavailability of coenzyme Q10 in dogs by inclusion complexation with γ-cyclodextrin. Asian J Pharm 1: 95–102.

Kang BK, Lee SJ, Chon SK, Jeong SY, Yuk SH, Khang G, Lee HB, Cho SH (2004) Development of self-microemulsifying drug delivery systems (SMEDDS) for oral bioavailability enhancement of simvastatin in beagle dogs. Int J Pharm 274: 65–73.

Kobayashi Y, Ito S, Itai S, Yamamoto K (2000) Physicochemical properties and bioavailability of carbamazepine polymorphs and dihydrate. Int J Pharm 193: 137–146.

Kommuru TR, Gurley B, Khan MA, Reddy IK (2001) Self-emulsifying drug delivery systems (SEDDS) of coenzyme Q10: formulation development and bioavailability assessment. Int J Pharm 212: 233–246.

Kwon SS, Nam YS, Lee JS, Ku BS, Han SH, Lee JY, Chang IS (2002) Preparation and characterization of coenzyme Q10-loaded PMMA nanoparticles by a new emulsification process based on microfluidization. J Colloids Surf A 210: 95–104.

Lee WC, Tsai TH (2010) Preparation and characterization of liposomal coenzyme Q10 for *in vivo* topical application. Int J Pharm 395: 78–83.

Li L, Pabbisetty D, Carvalho P, Avery MA, Avery BA (2008) Analysis of CoQ10 in rat serum by ultra-performance liquid chromatography mass

spectrometry after oral administration. J Pharma Biomed Analysis 46: 137–142.

Nehilla BJ, Bergkvist M, Popat KC, Desai TA (2008) Purified and surfactant-free coenzyme Q10-loaded biodegradable nanoparticles. Int J Pharm 348: 107–114.

Nepal PR, Han HK, Choi HK (2010) Enhancement of solubility and dissolution of Coenzyme Q10 using solid dispersion formulation. Int J Pharm 383: 147–153.

Palamakula A, Khan MA (2004) Evaluation of cytotoxicity of oils used in coenzyme Q10 Self-Emulsifying Drug Delivery Systems (SEDDS). Int J Pharm 273: 63–73.

Pardeike J, Schwabe K, Müller RH (2010) Influence of nanostructured lipid carriers (NLC) on the physical properties of the Cutanova Nanorepair Q10 cream and the *in vivo* skin hydration effect. Int J Pharm 396: 166–173.

Patravale VB, Date AA, Kulkarni RM (2004) Nanosuspensions: a promising drug delivery strategy. J Pharm Pharmacol 56: 827–840.

Pepe S, Marasco SF, Haas SJ, Sheeran FL, Krum H, Rosenfeldt FL (2007) Coenzyme Q10 in cardiovascular disease. Mitochondrion 7S: 154–167.

Teeranachaideekul V, Souto EB, Junyaprasert VB, Müller RH (2007) Cetyl palmitate-based NLC for topical delivery of Coenzyme Q10-Development, physicochemical characterization and in vitro release studies. Eur J Pharm Biopharm 67: 141–148.

Terao K, Nakata D, Fukumi H, Schmid G, Arima H, Hirayama F, Uekama K (2006) Enhancement of oral bioavailability of coenzyme Q10 by complexation with γ-cyclodextrin in healthy adults. Nutr Res 26: 503–508.

Tian F, Sandler N. Aaltonen J, Lang C, Saville DJ, Gordon KC Strachan CJ, Rantanen J, Rades T (2007) Influence of polymorphic form, morphology, and excipient interactions on the dissolution of carbamazepine compacts. J Pharm Sci 96: 584–594.

Thanatuksorn P, Kawai K, Hayakawa M, Hayashi M, Kajiwara K (2009) Improvement of the oral bioavailability of coenzyme Q10 by emulsification with fats and emulsifiers used in the food industry. Food Sci Tech 42: 385–390.

Zhang J, Wang S (2009) Topical use of Coenzyme Q10-loaded liposomes coated with trimethyl chitosan:Tolerance, precorneal retention and anticataract effect. Int J Pharm 372: 66–75.

Zhang Y, Aberg F, Appelkvist EL, Dallner G, Ernster L (1995) Uptake of dietary coenzyme Q supplement is limited in rats. J Nutrition 125: 446–453.